DYNAMICS OF ESSENTIALLY NONLINEAR VIBRATION ABSORBER COUPLED TO HARMONICALLY EXCITED 2 DOF SYSTEM

Yuli Starosvetsky
Faculty of Mechanical Engineering
Technion – Israel Institute of Technology
Technion City, Haifa, 32000, Israel
staryuli@tx.technion.ac.il

Oleg Gendelman[+]
Faculty of Mechanical Engineering
Technion – Israel Institute of Technology
Technion City, Haifa, 32000, Israel
ovgend@tx.technion.ac.il

Abstract

This paper investigates mitigation of vibrations in 2 DOF forced linear system with nonlinear energy sink (NES) attached. It is shown that analytic methods developed recently for description of periodic and strongly modulated response regimes in the two DOF harmonically excited systems (containing NES) may be successfully applied for 3 DOF system. Ability of the properly tuned NES to successfully absorb energy for each excited mode of the linear subsystem is demonstrated. Proposed methodology of the NES tuning guidelines is based on the analytical treatment developed for the system under investigation. Essentially nonlinear vibration absorber is compared to the best tuned linear one and excitation zones of preference of the nonlinear absorber are revealed.

Keywords: Nonlinear energy sink, strongly modulated regime, essentially nonlinear vibration absorber

1 Introduction

The most popular solution in a vibration isolation design is a linear vibration absorber, where an additional linear degree of freedom is added to the existing linear or weakly nonlinear system for the purpose of attenuating vibration over a narrow frequency range centered at the natural frequency of the absorber [Den Hartog J.P. (1956)].

Resent works [Gendelman O.V. (2001); Gendelman O.V., Vakakis A.F., Manevitch L.I. and McCloskey R., (2001); Vakakis A.F. and Gendelman O.V. (2001); Vakakis A.F. (2001); Vakakis A.F., Manevitch L.I., Gendelman O., Bergman L. (2003); Gendelman O.V. (2004); Gendelman O.V., Starosvetsky Y. (2006); O.V. Gendeman, Y.Starosvetsky, M. Feldman (2007); Y. Starosvetsky , O.V.Gendelman, (2007); E. Gourdon, N.A. Alexander, C.A. Taylor, C.H. Lamarque, S. Pernot (2007)] has motivated us to extend an analytical and numerical treatment to a harmonically excited 3-dof system (including NES attached). The structure of the paper is as follows. The second section is devoted to model description. Section three brings an analytical treatment including periodic regimes and strongly modulated response (SMR) description. Section 4 is fully based on the analytical treatment developed in section three and provides NES tuning guidelines. Section 5 contains numerical verifications of the analytical model and also studies effectiveness of the NES compared to the linear vibrations absorber. Section 6 contains concluding remarks and discussion.

2 Model

The system considered in the present paper consists of harmonically excited two-dof system of linear coupled oscillators (with identical masses) and nonlinear energy sink (NES) attached to it. By the term nonlinear energy sink we mean a small mass (relative to the linear oscillator mass) attached via strongly nonlinear spring (pure cubic nonlinearity) and linear viscous damper to the linear subsystem as it is illustrated at Fig.1.
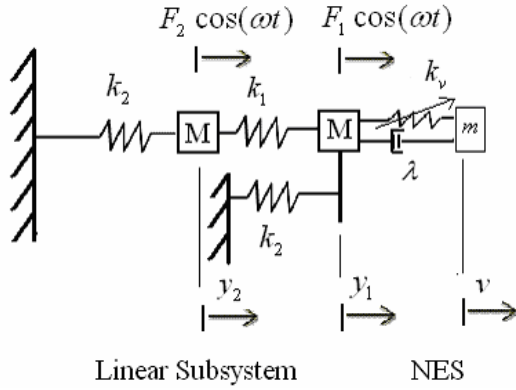
Figure 1. Mechanical model of the system

As it was mentioned above masses of linear oscillators are identical. The general system is described by the following equations:

$$M\ddot{y}_2 + k_2 y_2 + k_1(y_2 - y_1) = F_2 \cos(\omega t)$$
$$M\ddot{y}_1 + k_2 y_1 + k_1(y_1 - y_2) + k_v(y_1 - v)^3 + \quad (1)$$
$$+ \lambda(\dot{y}_1 - \dot{v}) = F_1 \cos(\omega t)$$
$$m\ddot{v} + k_v(v - y_1)^3 + \lambda(\dot{v} - \dot{y}_1) = 0$$

where y_1, y_2, v are the displacements of the linear oscillators and NES respectively, λ is the damping coefficient, F_i $(i = 1, 2)$ are the amplitudes of excitation of each linear oscillator. System (1) may be rescaled in the following way:

$$\tau = \sqrt{k_1/M}\, t; \quad \frac{d}{dt} = \sqrt{k_1/M}\, \frac{d}{d\tau}; \quad \tilde{\lambda} = \frac{\lambda}{\sqrt{Mk_1}}$$

$$y_1 = \frac{\tilde{k}_v \tilde{y}_1}{\sqrt{k_v/k_1}}; \quad y_2 = \frac{\tilde{k}_v \tilde{y}_2}{\sqrt{k_v/k_1}}; \quad v = \frac{\tilde{k}_v \tilde{v}}{\sqrt{k_v/k_1}} \quad (2)$$

$$\tilde{k}_2 = \frac{k_2}{k_1}; \quad \tilde{F}_i = \frac{\sqrt{k_v/k_1}}{\tilde{k}_v} \frac{F_i}{k_1}; \quad (i = 1, 2); \quad m/M = \varepsilon$$

Where $\tilde{k}_v$ is an arbitrary, non-dimensional coefficient. Substitution of (2) into (1) yields the following non-dimensional set:

$$\tilde{y}_2'' + (\tilde{k}_2 + 1)\tilde{y}_2 - \tilde{y}_1 = \tilde{F}_2 \cos(\Omega t)$$
$$\tilde{y}_1'' + (\tilde{k}_2 + 1)\tilde{y}_1 - \tilde{y}_2 = \tilde{F}_1 \cos(\Omega t) -$$
$$\qquad - \tilde{k}_v(\tilde{y}_1 - \tilde{v})^3 - \tilde{\lambda}(\tilde{y}_1' - \tilde{v}') \quad (3)$$
$$\varepsilon \tilde{v}'' + \tilde{k}_v(\tilde{v} - \tilde{y}_1)^3 + \tilde{\lambda}(\tilde{v}' - \tilde{y}_1') = 0$$

Where: $\Omega = \dfrac{\omega}{\left(\sqrt{k_1/M}\right)}$

Prime denotes the differentiation with respect to τ. $\varepsilon \ll 1$ is a small, non-dimensional parameter which establishes the order of magnitude for external excitation, damping, coupling and mass of the NES which is adopted to be ($m/M = \varepsilon$). By setting

$$\tilde{k}_v = \varepsilon\tilde{\tilde{k}}_v; \quad \tilde{F}_i = \varepsilon\tilde{\tilde{F}}_i; \quad \tilde{\lambda} = \varepsilon\tilde{\tilde{\lambda}} \text{ system} \quad (3)$$

transforms to:

$$\tilde{y}_2'' + (\tilde{k}_2 + 1)\tilde{y}_2 - \tilde{y}_1 = \varepsilon\tilde{\tilde{F}}_2 \cos(\Omega t)$$
$$\tilde{y}_1'' + (\tilde{k}_2 + 1)\tilde{y}_1 - \tilde{y}_2 = \varepsilon\tilde{\tilde{F}}_1 \cos(\Omega t) -$$
$$\qquad - \varepsilon\tilde{\tilde{k}}_v(\tilde{y}_1 - \tilde{v})^3 - \varepsilon\tilde{\tilde{\lambda}}(\tilde{y}_1' - \tilde{v}') \quad (3a)$$
$$\varepsilon \tilde{v}'' + \varepsilon\tilde{\tilde{k}}_v(\tilde{v} - \tilde{y}_1)^3 + \varepsilon\tilde{\tilde{\lambda}}(\tilde{v}' - \tilde{y}_1') = 0$$

Two natural frequencies of the linear oscillators are assumed in the work as incommensurate, remote (distance between dimensionless frequencies is of order O(1)) and fixed. Therefore the value of spring stiffness $\tilde{k}_2$ was picked in a way to provide two distinct incommensurate natural frequencies. Thus,

taking $\tilde{k}_2 = 1$ one obtains the following natural frequencies $\omega_2 = \sqrt{3}, \omega_1 = 1$.

Modal coordinates are introduced according to the following relationship:

$$\tilde{y}_1 = \frac{1}{\sqrt{2}}\left(x_1 + x_2\right) \; ; \; \tilde{y}_2 = \frac{1}{\sqrt{2}}\left(x_1 - x_2\right) \quad (4)$$

Transforming (3) into modal coordinates and performing additional rescaling one obtains:

$$\tilde{x}_2'' + 3\tilde{x}_2 = -\tilde{\varepsilon}\tilde{A}_2 \cos(\omega t) - \tilde{\varepsilon}\tilde{k}_v\left(\tilde{x}_1 + \tilde{x}_2 - v\right)^3 -$$
$$- \tilde{\varepsilon}\tilde{\lambda}\left(\tilde{x}_1' + \tilde{x}_2' - v'\right)$$

$$\tilde{x}_1'' + \tilde{x}_1 = \tilde{\varepsilon}\tilde{A}_1 \cos(\omega t) - \tilde{\varepsilon}\tilde{k}_v\left(\tilde{x}_1 + \tilde{x}_2 - v\right)^3 - \qquad (5)$$
$$- \tilde{\varepsilon}\tilde{\lambda}\left(\tilde{x}_1' + \tilde{x}_2' - v'\right)$$

$$\tilde{\varepsilon}v'' + \tilde{\varepsilon}\tilde{k}_v(v - \tilde{x}_1 + \tilde{x}_2)^3 + \tilde{\varepsilon}\tilde{\lambda}(v' - \tilde{x}_1' + \tilde{x}_2') = 0$$

Where:

$$\tilde{A}_1 = \tilde{\tilde{F}}_1 + \tilde{\tilde{F}}_2, \; \tilde{A}_2 = \tilde{\tilde{F}}_1 - \tilde{\tilde{F}}_2,$$
$$\tilde{x}_1 = \frac{x_1}{\sqrt{2}}; \tilde{x}_2 = \frac{x_2}{\sqrt{2}}; \tilde{\varepsilon} = \frac{\varepsilon}{2}$$

For the sake of convenience all the tilde marks are omitted.

3 System Regimes

Dynamic responses of a linear oscillator coupled to a nonlinear energy sink (NES) under harmonic forcing in the regime of 1:1:1 resonance have been studied in details [O.V. Gendeman, Y.Starosvetsky, M. Feldman (2007); Y. Starosvetsky , O.V.Gendelman, (2007)]. In the current paper we don't bring the detailed analytical treatment developed by O.V.Gendelman, (2006). However, it is essential to note that due to the fact that the natural frequencies of the linear substructure are remote and incommensurate the model can be reduced in the vicinity of each excited mode to yield the two-dof system treated in details in [Y. Starosvetsky , O.V.Gendelman, (2007)]. Thus, the previously developed analysis can be applied for the system under consideration.

Applying the analysis developed in [Y. Starosvetsky , O.V.Gendelman, (2007)] we are able to depict periodic, quasi-periodic and strongly modulated response regimes. We begin with the description of the simple periodic regimes. Performing the following changes of variables (in the vicinity of the first excited mode):

$$x_1 + x_2 - v \rightarrow w$$
$$x_1' + ix_1 = \varphi_1 \exp(i\tau)$$
$$x_2' + ix_2 = \varphi_2 \exp(i\tau) \qquad (6)$$
$$w' + iw = \varphi_w \exp(i\tau)$$

Introducing (6) into (5) and performing averaging over one forcing period it is possible to bring the system to the following form of autonomous, averaged equations:

$$\dot{\varphi}_2 + i(\varepsilon\sigma - 1)\varphi_2 = \frac{-\varepsilon A_2}{2} + \frac{3\varepsilon}{8}ik_v\left|\varphi_w\right|^2\varphi_w - \frac{\varepsilon\lambda}{2}\varphi_w$$

$$\dot{\varphi}_1 + i\varepsilon\sigma\varphi_1 = \frac{\varepsilon A_1}{2} + \frac{3\varepsilon}{8}ik_v\left|\varphi_w\right|^2\varphi_w - \frac{\varepsilon\lambda}{2}\varphi_w$$

$$\dot{\varphi}_w + i\left(\frac{1}{2} + \varepsilon\sigma\right)\varphi_w - \frac{3i}{2}\varphi_2 - \frac{i}{2}\varphi_1 = \frac{\varepsilon(A_1 - A_2)}{2} + \qquad (7)$$

$$+ (1 + 2\varepsilon)\frac{3}{8}ik_v\left|\varphi_w\right|^2\varphi_w - (1 + 2\varepsilon)\frac{\lambda}{2}\varphi_w$$

Taking $\dot{\varphi}_1 = \dot{\varphi}_2 = \dot{\varphi}_w = 0$ in (7) one derives the frequency response curves of periodic regimes. Corresponding frequency response diagrams are illustrated as the magnitude of φ_w vs. frequency of excitation (Fig.2).
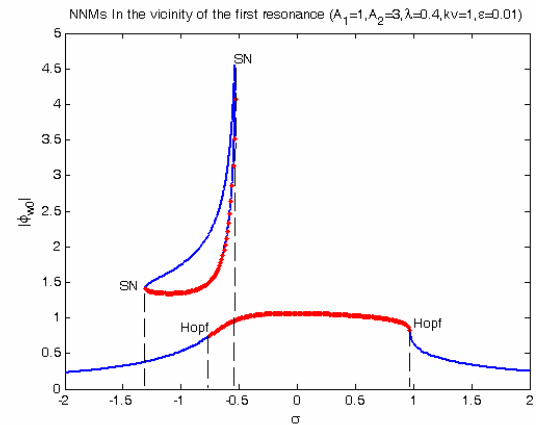
Figure 2. Frequency response diagram in the vicinity of the first excited mode. Blue lines refer to the stable periodic responses when the red ones refer to the unstable ones. System Parameters: $A_1 = 1, A_2 = 3, \lambda = 0.4, k_v = 1, \varepsilon = 0.01$

Frequency response diagram for the second excited mode is obtained in the similar manner and is illustrated on Fig. 3.
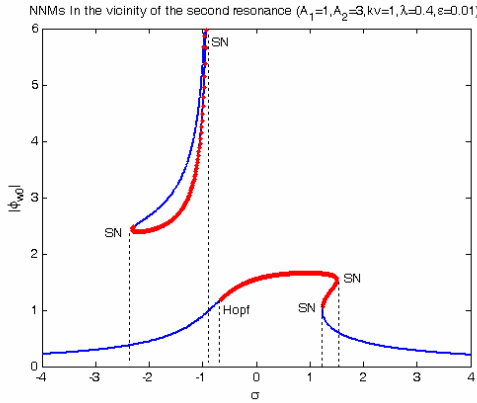
Figure 3. Frequency response diagram in the vicinity of the second excited mode. Blue lines refer to the stable periodic responses when the red ones refer to the unstable ones. System Parameters: $A_1 = 1, A_2 = 3, \lambda = 0.4, k_v = 1, \varepsilon = 0.01$

Saddle node and Hopf bifurcations were revealed by the stability analysis. They are marked on the frequency response diagrams (Figs. 2-3).

Additional system response is referred to as a strongly modulated response (SMR). Further analytical treatment of the SMR will be briefly presented in the vicinity of the first excited mode. Since the natural frequencies are remote and we are considering the excitation in the vicinity of the first mode thus the influence of the second (unexcited) mode can be omitted. This can be derived straightforwardly from the asymptotic analysis performed. Therefore considering the following change of variables:

$$u = x_1 + \varepsilon v, \varphi_u \exp(it) = \dot{u} + iu$$
$$w = x_1 - v, \varphi_w \exp(it) = \dot{w} + iw \quad (8)$$

Substitution of (8) into (5) and averaging over one forcing period yields:

$$\varphi_u' + i\varepsilon\sigma\varphi_u + \frac{i\varepsilon}{2(1+\varepsilon)}(\varphi_u - \varphi_w) = \frac{\varepsilon A_1}{2}$$

$$\varphi_w' + i\varepsilon\sigma\varphi_w + (1+\varepsilon)\frac{\lambda}{2}\varphi_w + \frac{i}{2(1+\varepsilon)}(\varphi_w - \varphi_u) \quad (9)$$

$$+ k_v(1+\varepsilon)\left(\frac{-3i(1+\varepsilon)}{8}|\varphi_w|^2\varphi_w + \varepsilon\langle 3w^2 x_2\rangle\right) = \frac{\varepsilon A_1}{2}$$

It is apparent from system (9) that the averaged part of an unexcited mode (x_2) enters the equations (9) in epsilon order and it doesn't affect the system dynamics in the leading approximation. Since in the analysis presented in [Y. Starosvetsky , O.V.Gendelman, (2007)] for both fast and slow regions of system evolution only the leading approximation was used, therefore further treatment of (9) remains similar to this of [Y. Starosvetsky , O.V.Gendelman, (2007)]. In this paper we use the developed earlier analysis in order to estimate the regions of the SMR existence in the frequency domain (for each excited mode).

As it was demonstrated earlier introducing two time scales ($t-$ fast and $\tau = \varepsilon t -$ slow) and applying multiple scales analysis it is possible to derive the slow invariant manifold (SIM) on which the system exists when exhibiting the slow type motion.

$$(\frac{i}{2}\varphi_2 + \frac{\lambda}{2}\varphi_2 - \frac{i}{2}|\varphi_2|^2\varphi_2) = C(\tau,...) \quad (10)$$

Further multiple scales expansion provides another set of differential equations describing the system dynamics on the SIM.

$$\left[\frac{\lambda}{2} - \frac{i}{2} + i|\varphi_2|^2\right]\frac{\partial\varphi_2}{\partial\tau} - \frac{i}{2}\varphi_2^2\frac{\partial\varphi_2}{\partial\tau} = G$$

$$G = -\frac{1-\sigma}{4}|\varphi_2|^2\varphi_2 - \left[\frac{\sigma}{4} + \frac{i\lambda(1-\sigma)}{4}\right]\varphi_2 + \frac{iA}{4} \quad (11)$$

Presenting φ_2 in the form ($\varphi_2 = |\varphi|\exp(i\theta)$) we draw a phase portrait (Fig. 4).
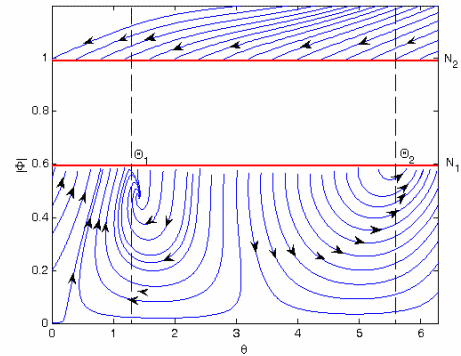
Figure 4. Phase portrait of the slow invariant manifold

The region above N_2 and the region below N_1 on the phase portrait refer to the stable branches of SIM when the intermediate region ($N_1 < N < N_2$) refers to the unstable one. Therefore the slow system evolution is depicted on these regions.

Observing the phase portrait presented at Fig. 4 we can see that there is an interval of θ - [$\Theta_1 < \theta < \Theta_2$] for which all the phase trajectories are repelled from the lower fold N_1 ($|\Phi| = N_1$). In the regime of the relaxation oscillations, the phase trajectory jumps from a point of this interval to the upper branch of the SIM, then it moves along the line of the slow flow to the upper fold line, then jumps back to the lower branch and moves to the lower fold line, commencing in one of the points of the interval $[\Theta_1, \Theta_2]$ in order to enable the next jump. Therefore it is natural to consider this regime as mapping of the interval $[\Theta_1, \Theta_2]$ into itself – the regime of the relaxation oscillations will correspond to attractor of this one – dimensional map.

In order to build the relevant mapping, we should consider separately the "slow" and the "fast" parts of the mapping cycle. As for the "slow" parts on the lower and the upper branches of the SIM, we can use equations (11) and directly connect the "entrance" and "exit" points. Due to complexity of the equations, this part of the mapping should be accomplished numerically. As for the "fast" parts, the function φ₂ should be continuous at the points of contact between the "fast" and the "slow" parts. Therefore, for "fast" parts of the motion one obtains complex invariant C(τ₁), defined by Equation (10). If one knows its value at the point of "start", it is possible co compute N and θ for the point of "finish" unambiguously and thus to complete the mapping. The procedure of numerical integration should be performed twice – for two branches of the SIM. Two invariants

should be computed for two "fast" jumps, in order to determine their final points.

Not every trajectory which starts from the lower fold of the SIM will reach the initial interval since it may be attracted to alternative attractor at the upper or the lower branch of the SIM, if it exists. Of course, only those points which are mapped into the interval can carry sustained relaxation oscillations. The mapping procedure is illustrated at Figs. 5-6
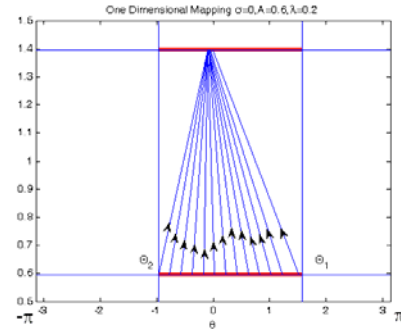
Figure 5 One dimensional mapping;
$\sigma = 1, A = 0.6, \lambda = 0.2$.
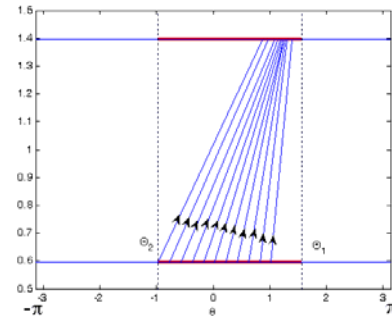
Figure 6 One dimensional mapping;
$\sigma = 2.9, A = 0.6, \lambda = 0.2$.

. The mapping at Fig. 5 exists for all points of the interval and is obviously contractive. Therefore one can expect existence of stable attractor corresponding to the regime of the relaxation oscillations (or SMR). By increasing the detuning parameter value (Fig. 6) one can notice that the mapping lines tend to the right and there is also a region on the basin which doesn't contain any lines. This region relates to the unaccomplished cycles, namely to the phase trajectories which started from the region and have been attracted to the periodic response attractor before they have reached the

basin one more time. The mentioned trajectories are not illustrated on the diagram. It is clear from Fig. 6 that there is no stable attractor of the SMR and for every initial condition on the basin the system finally (after sufficient number of cycles) leaves the basin.

By now we can conclude that for some increased values of detuning parameter the SMR attractor vanishes.

Running with the values of detuning (σ) and for each step performing the mapping one can track the value of σ for which the attractor vanishes. This provides a general tool for determination of the frequency region for the existence of strongly modulated response.

As it was stressed above we are able to apply the developed earlier analysis by reduction of the system in the vicinity of each mode. Therefore, using the procedure based on one dimensional mapping diagram we are capable to estimate analytically the frequency intervals for the region of SMR existence. Let us consider the following frequency response diagrams (Fig. 7) in the vicinity of each excited mode.
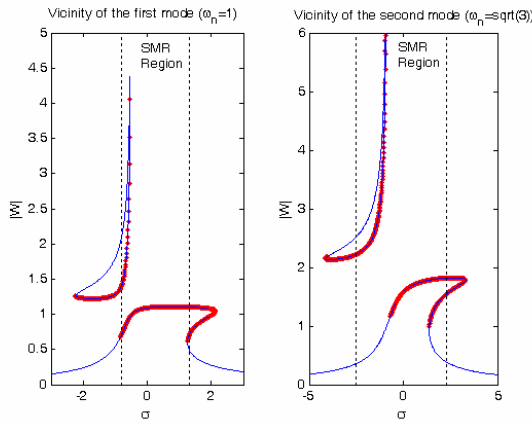
Figure 7 Frequency response diagrams. Frequency region of SMR existence is marked with the dashed lines. Blue lines refer to the stable periodic responses when the red ones refer to the unstable ones. System Parameters: $A_1 = 1, A_2 = 3, \lambda = 0.2, k_v = 1, \varepsilon = 0.01$

The left diagram of Fig. 7 corresponds to the first excited mode ($\omega_n = 1$) when the right diagram

corresponds to the second one ($\omega_n = \sqrt{3}$). Favorable regimes in a sense of vibration mitigation are periodic and quasi-periodic ones (related to the lower branch of periodic regimes) and also SMR. As we can see from the diagrams there is also an undesired response related to the upper branch of the periodic regimes. Designing the properly tuned NES we should take the undesired responses into consideration, trying to avoid or at least weaken the undesired response as much as possible.

4 NES Tuning Guidelines

Main guidelines of nonlinear vibration absorber tuning will be presented in current section. Tuning procedure is based on the analytical treatment results of previous section. As it was shown in [Y. Starosvetsky, O.V.Gendelman, (2007)] strongly modulated response can be much more effective from a point of view of vibration absorption then simple periodic one in the close vicinity of main resonance (1:1). Thus, the main goal of the tuning procedure is to allow excitation of the SMR in occurrence of each mode for the same attached NES (without changing NES parameters). This situation may be realized in various engineering applications when linear structure undergoes harmonic loading in a wide range of the excitation frequencies. Thus there is a need for a protection of the system in the whole range of excitation frequency including both dangerous modes. We will demonstrate the tuning procedure concept by considering the following example.

Example 1

Let us consider the following parameters of excitation amplitudes and mass of the nonlinear absorber $A_1 = 1; A_2 = 3$, $m = \varepsilon = 0.01$ correspondingly. We need to find a pair of NES parameters (k_v, λ) which allows SMR excitation in the vicinity of each mode of linear subsystem. In order to find such a pair we actually change NES parameters

(k_v, λ) with a small step and for each pair we construct the one dimensional maps in the occurrence of each excited mode. When we finally obtain a certain frequency ranges of SMR existence (stable attractor of the one dimensional map) about each excited mode we actually satisfied the base requirement of the tuning procedure. Say we have performed the described procedure and found a certain pair of $k_v = 1, \lambda = 0.2$ parameters which allows SMR excitement in the neighborhood of each mode. For this pair we are plotting frequency-response diagrams in the occurrence of each mode (Fig. 7). These diagrams consist of periodic regimes amplitudes and frequency range of existence of SMR calculated using one dimensional map approximation described in the previous section. Despite the excitement of the SMR in the vicinity of each mode one can note the dangerous situation in the neighborhood of the left bound of the SMR for the first excited mode. Observing the diagram of Fig. 7 for the first excited mode we can see Hopf bifurcation occurs on the lower stable branch slightly before the region of SMR existence (left bound). This bifurcation causes an undesired effect on the system response since the loss of stability by the lower branch may be accompanied by the jump to the upper stable branch which results in large vibration amplitudes. In order to avoid this effect we should attempt to translate Hopf bifurcation of the lower branch into the region of the SMR existence thus assuring continuation from lower stable branch regimes into SMR (without jumps to higher amplitudes). Therefore, increasing damping parameter from $\lambda = 0.2$ to $\lambda = 0.4$ we plot the same frequency response diagrams for each excited mode (Fig. 8). Frequency response diagrams presented on Fig. 8 suggest for the continuation between lower stable branch and SMR for both modes.

In the next section numerical simulation for the entire frequency range (including both modes) will be carried out for the systems with

zero initial conditions and it will be shown that there are no jumps to the upper branches.
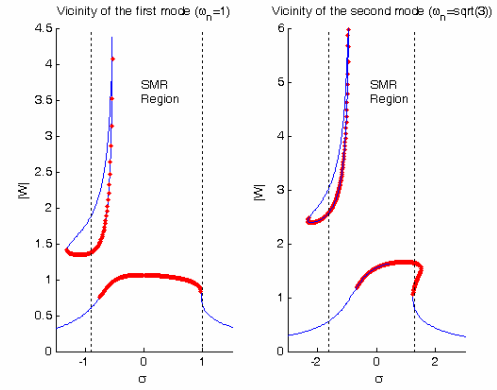
Figure 8 Frequency response diagrams in occurrence of each excited mode. SMR regions of existence calculated via one dimensional map are bounded by the dotted lines. Solid red lines refer to unstable solution when blue solid lines refer to the stable ones. System Parameters:
$$A_1 = 1, A_2 = 3, \lambda = 0.4, k_v = 1, \varepsilon = 0.01$$

It is essential to note that there is also a possibility for the upper stable branch regimes excitement by appropriate initial conditions. However it will be shown in the following section that those regimes may be excited only by high magnitudes of initial deflections relative to the amplitudes of an external forcing $(\varepsilon A_1, \varepsilon A_2)$. In the present work it is also assumed that an excited system doesn't suffer from strong additional excitations (e.g. impacts, pulses) which are definitely able to translate it to the upper branch.

Summarizing the results of an example provided above we have seen that it is not enough to excite SMR in the vicinity of both system modes, but it is also extremely important to follow after stability of the lower branch of periodic regimes amplitude. As soon as we manage to translate the bifurcation point of the lower branch of periodic response into the region of SMR existence we can enjoy the effectiveness of NES application in a 2-dof linear subsystem.

5 Numerical Simulations

In order to study NES performance we plot system response (for zero initial conditions)

vs. frequency of excitation in the entire frequency range, including both modes of the linear subsystem. System response is presented in terms of maximum linear subsystem energy like component ($\max(y_1^2 + y_2^2)$) vs. frequency of excitation Fig. (9a), maximal deflection of each dof of linear subsystem (y_1, y_2) vs. frequency of excitation (Fig. 9 b, c), mean amplitude deflection of each dof of linear subsystem vs. frequency of excitation (Fig. 9 d, e). On the same plots we also illustrate the response of an optimally tuned linear absorber. Linear absorber was tuned numerically according to the objective function of the minimal sum of two resonant peaks of the frequency response curve. System parameters for the following simulations

are: $A_1 = 1; A_2 = 3; k_v = 1; \lambda = 0.4; \varepsilon = 0.01$
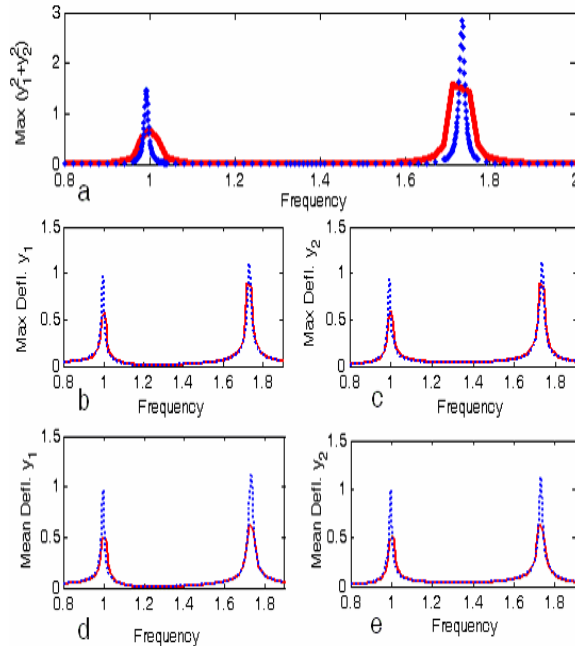
Figure 9 a) Linear subsystem energy like response vs. frequency of excitation; red bold line refers to the system response with NES attached when dotted blue line refers to the system response with tuned linear absorber attached. b, c) Maximal amplitude deflection of linear subsystem dofs; red bold line refers to the response with NES attached when dotted blue line refers to the response with tuned linear absorber attached. d, e) Mean amplitude deflection of linear subsystem dofs; red bold line

refers to the system response with NES attached when dotted blue line refers to the system response with tuned linear absorber attached.

We proceed with the numerical estimation of the parametric zones of external amplitudes of excitation for which SMR generated by NES is better then system response with best tuned linear absorber attached. Fig. 10 demonstrates dotes on a plane of external excitation (A_1, A_2) for which SMR is preferable on the responses of the system coupled to the tuned linear absorber.
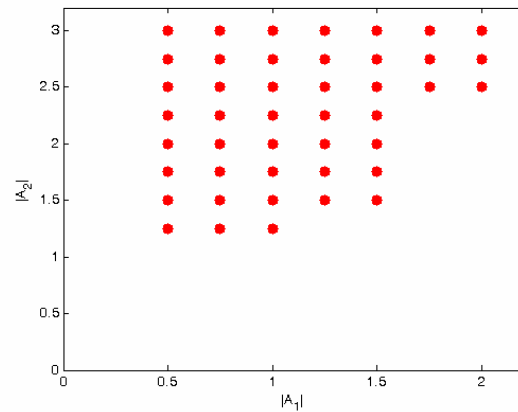
Figure 10 External excitation plane, dotes are related to those excitation amplitudes for which SMR is preferable on the response of system coupled to the tuned linear absorber.

Observing the results presented on Fig. 10 one can notice that preference of the SMR arises for the relatively high amplitudes of excitation. This result is not surprising at all since as it comes from the analytical model the upper branch of the SIM doesn't depend on the amplitude of excitation. Therefore for some low amplitudes of excitation SMR may be already excited however system response will be rather high comparing with the case of linear absorber application. In the case of high amplitudes of excitation system response with linear absorber attached will overcome the SMR response. This is due to the fact that SMR is weakly affected by the growth of the amplitude of excitation contrary to the case of linear absorber application.

In order to demonstrate the robustness of the periodic response regime related to the lower stable branch of the frequency response curves and strongly modulated response we have performed numerical integration for the random set of initial conditions. Thus, randomly picking 300 triples of initial deflections (x_{10}, x_{20}, v_0) in the following range $(-0.5 \leq (x_{10}, x_{20}, v_0) \leq 0.5)$ original system (5) was integrated numerically in the vicinity of each mode. Random data of initial conditions for which system (5) was integrated is presented on Fig. 11.
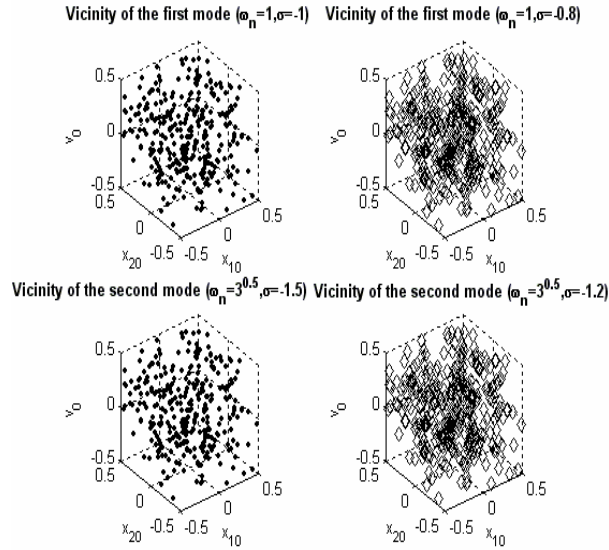
Figure 11 Random data of the initial deflections in the range $(-0.5 \leq (x_{10}, x_{20}, v_0) \leq 0.5)$.

For simulations for various values of frequency of excitation were performed. Each simulation was done for the random set of initial deflections data (initial velocities are set to zero) shown on Fig. 11. Two frequencies of excitation were picked for each mode. The first selected frequency refers to the region of two stable periodic regimes coexistence not including SMR. The second one refers to the region of coexistence of SMR together with stable periodic response related to the upper branch of frequency response curve. Frequencies of excitation are as follows:

| First mode: | $\omega=1+\varepsilon\sigma;$ | $(\sigma = -1, -0.8)$ |
| Second mode: | $\omega=\sqrt{3}+\varepsilon\sigma;$ | $(\sigma = -1.5, -1)$ |

System parameters:
$$A_1 = 1, A_2 = 3, \varepsilon = 0.01, \lambda = 0.4, k_v = 1$$

The results of the performed simulations are illustrated on Fig. 12. Each point of the random set of initial conditions is marked with respect to the type of the steady state response regime obtained by numerical integration started from this particular initial condition. Thus 'diamond' marker refers to SMR, 'dot' marker refers to the periodic regime of the lower stable branch and 'circle' marker refers to the one of the upper stable branch.
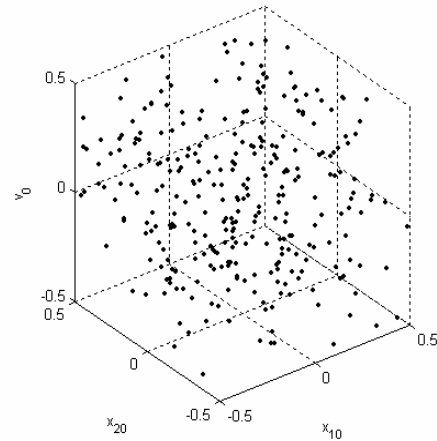
Figure 12 Initial conditions data for several frequencies of excitation. Dots are related to the periodic r response regime of the lower stable branch; Diamonds are related to the SMR

It is clear from the results brought on Fig. 12 that for the frequency of excitation in zone of the coexistence of two periodic regimes for both modes all the trajectories which correspond to the brought above initial conditions are attracted to the lower stable branch of periodic response regime. For the frequency of excitation in zone of the coexistence of SMR and periodic responses for both modes, all the trajectories corresponding to the same set of the initial conditions are attracted to the SMR. Obtained results provide additional confirmation of the robustness of the periodic regime related to the

lower stable branch and SMR in the vicinity of zero initial conditions. It is essential to note that the range of initial deflections is of magnitude which is much higher then the magnitude of the external excitation.

6 Conclusions

Considered system is comprised of harmonically forced two DOF linear subsystem (primary system) and essentially nonlinear attachment. It is shown that analytical methods developed in [Y. Starosvetsky , O.V.Gendelman, (2007)] for the description of periodic regimes and SMR may be successfully applied to the described three DOF system in case when modal frequencies are remote and incommensurate. Derived analytical model is used for estimation of system responses and guidelines for the nonlinear absorber tuning are formulated. As it comes from numerical simulations in some cases of high amplitudes of excitation nonlinear absorber may effectively absorb energy from the primary linear subsystem for both excited system modes. In these cases nonlinear absorber appears to be much more favorable then linear one. Thus summarizing the drawbacks of the essentially nonlinear vibration absorber we note its inefficiency for the low amplitudes of excitation and an existence of additional branch of periodic regimes with relatively high magnitude. However as it was demonstrated in the previous section the last drawback may be minimized by proper NES design and these regimes are not excited for the certain range of initial conditions. The magnitude of this range is much bigger then the amplitudes of an external excitation and thus provides a fairly good approximation to the real life applications.

Thus, each case of external loading should be revisited by the designer and proper absorber should be selected taking into account the whole packet of their advantages and drawbacks.

References

Den Hartog J.P. (1956) Mechanical Vibrations 4th edition , McGraw-Hill Book Company

Gendelman O.V. (2001) Transition of Energy to Nonlinear Localized Mode in Highly Asymmetric System of Nonlinear Oscillators, *Nonlinear Dynamics*, **25**, 237-253.

Gendelman O.V., Vakakis A.F., Manevitch L.I. and McCloskey R., (2001) Energy Pumping in Nonlinear Mechanical Oscillators I: Dynamics of the Underlying Hamiltonian System, *Journal of Applied Mechanics*, **68**, n.1, 34-41.

Gendelman O.V. (2004) Bifurcations of Nonlinear Normal Modes of Linear Oscillator with Strongly Nonlinear Damped Attachment, *Nonlinear Dynamics,* v.37, n.2, pp.115-128

Gendelman O.V., Starosvetsky Y. (2006) Quasiperiodic Response Regimes of Linear Oscillator Coupled to Nonlinear Energy Sink Under Periodic Forcing, in press, *Journal of Applied Mechanics*

Vakakis A. F., Manevitch L. I., Mikhlin Yu. V., Pilipchuk V. N., and Zevin A. A. (1996) *Normal Modes and Localization in Nonlinear Systems*, Wiley Interscience, New York.

Vakakis A.F. and Gendelman O.V. (2001) Energy Pumping in Nonlinear Mechanical Oscillators II: Resonance Capture, *Journal of Applied Mechanics*, **68**, n.1, 42-48.

Vakakis A.F. (2001) Inducing passive nonlinear energy sinks in linear vibrating systems Journal *of Vibration and Acoustics* **123**(3), 324-332.

Vakakis A.F., Manevitch L.I., Gendelman O., Bergman L. (2003) Dynamics of Linear Discrete Systems Connected to Local Essentially Nonlinear Attachments. *Journal of Sound and Vibration*, **264**, 559-577

Gendeman O.V., Y.Starosvetsky, M. Feldman (2007) Attractors of Harmonically Forced Linear Oscillator with Attached Nonlinear Energy Sink I: Description of Response Regimes, in press, *Nonlinear Dynamics*

Y. Starosvetsky , O.V. Gendelman (2007), Attractors of Harmonically Forced Linear Oscillator with Attached Nonlinear Energy Sink II: Optimization of a Nonlinear Vibration Absorber , in press, *Nonlinear Dynamics*

Y. Starosvetsky and O.V.Gendelman (2007), Strongly modulated response in forced 2DOF oscillatory system with essential mass and potential asymmetry, accepted for publication in, *Phisica D*

Y. Starosvetsky and O.V.Gendelman (2007), Dynamics of a strongly nonlinear vibration absorber coupled to a harmonically excited two-degree-of-freedom system, accepted for publication in *Journal of Sound and Vibration*

E. Gourdon, N.A. Alexander, C.A. Taylor, C.H. Lamarque, S. Pernot (2007), Nonlinear energy pumping under transient forcing with strongly nonlinear coupling: Theoretical and experimental results, *Journal of Sound and Vibration* 300 (2007) 522-551